Scripta Materialia 117 (2016) 11–15

Contents lists available at ScienceDirect

Scripta Materialia

journal homepage: www.elsevier.com/locate/scriptamat

Do defects get ordered in Cu_2ZnSnS_4?

Sunil Kumar Samji, Ramanjaneyulu Maanam, M.S. Ramachandra Rao

Department of Physics and Nano Functional Materials Technology Centre, Indian Institute of Technology Madras, Chennai 600036, India

ARTICLE INFO

Article history:
Received 15 January 2016
Accepted 6 February 2016
Available online xxxx

Keywords:
Cu_2ZnSnS_4
Ordered defect compounds
XPS
Grain boundary physics
C-AFM

ABSTRACT

Formation of ordered defect compounds and anomalous grain boundary physics are unique to Cu chalcogenides $CuInX_2$ (S/Se) and its alloys. X-ray photoelectron spectroscopy (XPS) studies were carried on $Cu_{2-x}Zn_{1.3}SnS_4$ (x = 0.0, 0.3, 0.5 and 0.7) to determine the position of valence band edge and explore the formation of ordered vacancy compounds along with absorption studies. Conductive atomic force microscopy (C-AFM) studies were carried out Cu_2ZnSnS_4 (CZTS) film deposited on Si and sodalime glass substrates to understand grain boundary physics.

CdTe, $CuInSe_2$ (CIS), $CuInGaSe_2$ (CIGS) and Cu_2ZnSnS_4 (CZTS) belong to the family of chalcogenide semiconductors and the last three to Cu based chalcogenides. While CIGS belongs to ternary group of Cu chalcogenide, CZTS belongs to quaternary system. CIGS solar cells have been reported to show an efficiency of 21.7% and CZTS solar cells an efficiency of 12.6% [1,2]. CIGS and CZTS have several similarities, yet striking differences that limit their performance. Both belong to the family of Cu chalcogenides, have high absorption coefficient in the visible region of the solar spectrum and direct nature of the bandgap. Both are polar semiconductors and display unique grain boundary (GB) physics with high device efficiency under non-stoichiometric conditions [3–5]. However, there are equally strong reasons/differences explaining as to why CZTS devices fall short of the performance compared to ternary counterparts [6,7]. CZTS has a very narrow window region of the phase diagram within which phase purity can be obtained [8]. Deviation from stoichiometry results in precipitation of secondary phases [9]. High efficiency is reported under Cu-poor and Zn-rich conditions while precipitation of ZnS is one of the well reported problems under Zn-rich conditions that is highly detrimental to device performance [3,10,11]. Guo et al. reported an efficiency of 0.23% under stoichiometric conditions and an efficiency of 7.23% under non stoichiometric conditions [12,13] which is a staggering hike in efficiency. The fundamental mechanism for the huge hike in efficiency is not yet understood. In CIGS and CZTS devices, Molybdenum (Mo) acts as a back electrode and a *p–n* junction are formed between CIGS (CZTS) and CdS. In the case of CZTS, a detrimental reaction between the absorber layer CZTS and the back electrode Mo layer takes place giving rise to secondary phases at the interface which hinder the device performance [14]. Defect physics *i.e.* formation of ordered vacancy compounds and anomalous GB physics are unique to Cu chalcogenides [15–18]. However, these properties are not extensively studied in quaternary systems (kesterites) as in ternary chalcogenides. The present work discusses defect physics *i.e.* possibility of formation of ordered vacancy compounds as well as GB physics in quaternary systems.

Due to the polar nature of $CuInSe_2$ and its alloy $CuInGaSe_2$, a thin layer is spontaneously formed in order to neutralize the charge created by the dipoles. This spontaneously formed layer is typically *n*-type in nature and hence forms a homo-epitaxial *p–n* junction between chalcogenide CIGS (which is intrinsically *p*-type) and defect chalcopyrite layer, in addition it provides better band alignment and device performance. This top defective layer is called an ordered defect compound [18,19].

A perfectly crystalline solid is a highly ordered system defined by translation symmetry *i.e.* long range ordering. However, in reality materials contain defects which break symmetry, *i.e.* creation of defects introduces disorder. In certain cases where there are enough defects, the defects themselves tend to get ordered which is observed in $CuInSe_2$ and such systems are called ordered defect/vacancy compounds. Chalcogenide semiconductors such as $CuInSe_2$ exhibit formation of ordered vacancy compounds *viz.* $CuIn_5Se_8$, $CuIn_3Se_5$ and $Cu_2In_4Se_7$ obtained by repeating m (m = 1) units of $[2V_{Cu}^{-} + In_{Cu}^{2+}]$ defect pairs over n units of $CuInSe_2$ (formula unit) [16,19]. The ordered vacancy compounds form a layer on the surface of the semiconductor and typically are n-type semiconductors, whereas, $CuInSe_2$ is a p-type semiconductor. Hence an epitaxial homo *p-n* junction is formed between $CuInSe_2$ and OVCs. This also provides a better band alignment and improves the efficiency of the device [16,18]. This is well studied in ternary compounds [19] while in quaternary semiconductors, studies are scarcer. Du et al. reported surface photovoltage measurements on CIGS, CZTS and CZTSSe films, where non-linearity in the current was reported only in case of CIGS which was attributed to type inversion

E-mail address: suniliitm@gmail.com (S.K. Samji).

http://dx.doi.org/10.1016/j.scriptamat.2016.02.009
1359-6462/

(formation of ordered vacancy compounds) in CIGS and absent in case of CZTS and CZTSSe [20]. Another way to explore the formation of OVCs is by X-ray photoelectron spectroscopy (XPS). It is known that the formation of OVCs involves the creation of V_{cu} (both in chalcogenides and kesterites) on the surface. In ternary $CuInSe_2$ and quaternary CZTS compounds, the valence band is made up of Cu 3*d* electrons. When V_{cu} defects are formed on the surface, a shift in the valence band edge is anticipated, and this shift can be determined from x-intercept of the valence band edge of the XPS data.

Confirmation of formation of ordered vacancy compounds by XPS requires determination of position of valence band edge. In XPS studies Fermi level E_F corresponds to 0 eV. In an *n*-type semiconductor E_F lies near to conduction band edge and in case of p-type semiconductor it lies nearer to valence band edge. Cu Chalcogenides are intrinsically *p*-type and when an ordered vacancy compound is spontaneously formed, which is n-type a shift in the position of the valence band edge takes place [18]. The separation between Fermi level and valence band edge $|E_F - E_V|$ in an n-type semiconductor is of the order of bandgap (approximately equal to bandgap), whereas in p-type semiconductor, it is relatively small compared to bandgap. XPS studies were carried on $Cu_{2-x}Zn_{1.3}SnS_4$ (x = 0.0, 0.3, 0.5 and 0.7) to determine $|E_F - E_V|$ and in the event of formation of OVCs, a $|E_F - E_V|$ comparable to bandgap of CZTS is anticipated.

Stoichiometric (Zn/Sn = 1) as well as Cu-poor and Zn-rich CZTS thin films with nominal composition $Cu_{2-x}Zn_{1.3}SnS_4$ (x = 0, 0.3,0.5 and 0.7) were prepared using nano-ink by drop casting it on a glass substrate and heating it at 350 °C for 1 h in N_2 atmosphere. High pure Copper (II) Acetate monohydrate (Sigma Aldrich), Zinc Acetate (Alfa aeser), Tin Chloride penta hydrate (Sigma Aldrich) and elemental sulfur (Sigma Aldrich) dissolved in oleylamine (Sigma Aldrich) were used as precursors for the synthesis of nano-ink. In the present work CZTS nano-ink was prepared from hot-injection technique. XPS measurements were carried out with Specs, Mg and *Kα* photons (1253.6 eV) have been used and XPS spectra were recorded at a pressure of 4×10^{-10} mbar by using Specs cylindrical mirror analyzer with pass energy of 30 eV. XPS measurements were carried out on CZTS thin films to obtain surface composition and explore the formation of ordered vacancy compounds. Absorption studies were carried out with Jobin Yvon spectrophotometer, C-AFM studies were carried out with Bruker dimension edge model SPM.

Survey scan spectra recorded on $Cu_{2-x}Zn_{1.3}SnS_4$ (x = 0, 0.3, 0.5 and 0.7) films in XPS studies are shown in the Fig. 1. XPS peaks corresponding to Cu, Zn, Sn and S are marked in the spectra.

From the XPS data, the valence band has been found to lie in the range 0–30 eV of binding energy. Valence band spectra for $Cu_{2-x}Zn_{1.3}SnS_4$ (x = 0.0, 0.3, 0.5 and 0.7) films are shown in the Fig. 2(i).

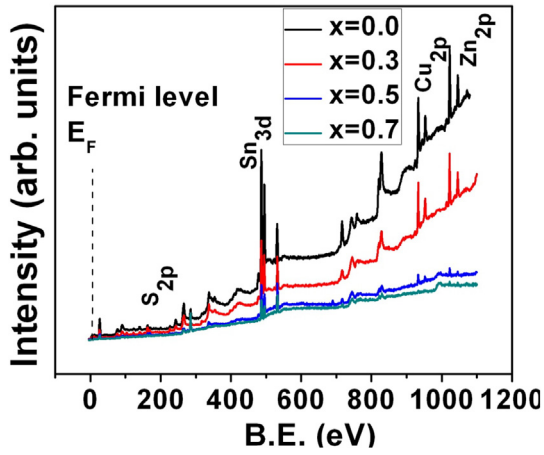

Fig. 1. XPS survey scan spectra recorded on $Cu_{2-x}Zn_{1.3}SnS_4$ (x = 0, 0.3, 0.5 and 0.7) films.

The portion highlighted corresponds to the edge of the valence band for each composition. The position of valence band is obtained from extrapolation of the linear fit of the data of valence band edge on the x-axis. The inset of the Fig. 2(i) shows, the position of the valence band edge for x = 0.3 and it is around 0.41 eV. The position of valence band edge determined for all x in $Cu_{2-x}Zn_{1.3}SnS_4$ (x = 0.0, 0.3, 0.5 and 0.7) are shown in the Fig. 2(ii).

The linear fit to valence band edge and its position is shown by a small arrow pointing to the x-axis as shown in Fig. 2(ii) (a)–(d). In case of formation of ordered vacancy compound in CZTS, the value of $|E_F - E_V|$ is expected to be around 1.5 eV or even more. In the case of Cu-poor and In-rich $CuInSe_2$ reported by Schmid et al. [18] $|E_F - E_V|$ is 1.3 eV whereas bandgap of $CuInSe_2$ is only 1.1 eV which was attributed $CuIn_3Se_5$, an ordered vacancy compound. Also a bandgap of 1.3 eV was reported by simulating the absorption spectrum of $CuIn_3Se_5$. This was reported under Cu-poor and In-rich conditions. Since in quaternary semiconductors, In is replaced by Zn and Sn (50% each) and in place of estimating In/(In + Cu) at the surface as a function of bulk composition, (Zn + Sn)/(Zn + Sn + Cu) is estimated and compared as against corresponding bulk value. (Zn + Sn)/(Zn + Sn + Cu) as determined from EDS data and XPS are listed along with $|E_F - E_V|$ and bandgaps for all x in $Cu_{2-x}Zn_{1.3}SnS_4$ in Table 1. It can be clearly observed from the table that for all x the (Zn + Sn)/(Zn + Sn + Cu) determined XPS are almost constant and the values vary little around 0.80 eV, this is similar to ternary $CuInSe_2$ where In/(In + Cu) surface composition remains constant with the change in Cu vacancies.

Fig. 3 Shows graph plotted between (Zn + Sn)/(Zn + Sn + Cu) determined from XPS and EDS. The graph resembles or has the same trend as that of In/(In + Cu) composition as reported by Schmid et al. *i.e.* in the bulk of the material, the samples are Cu/(Zn + Sn) poor while the surface is (Zn + Sn)/(Zn + Sn + Cu) rich.

Zhang et al. reported that there are different types of ordered vacancy compounds in $CuInSe_2$ that can be formed under Cu-poor and In-rich conditions and the actual ordered vacancy compound that is spontaneously formed on p-$CuInSe_2$ strongly depends on the density of Cu vacancies. Within a given formula unit ($CuInSe_2$), as the density of Cu vacancies changes the spontaneously formed OVC differs. This is highly relevant and important to the present scenario as the synthesized samples differ in their Cu stoichiometry and the actual form of OVC formed on each (corresponding to different x) may differ. However, there are two important points which need to be verified that corroborate the discussion: (a) when there is a change in the density of Cu vacancies, and the fact that the valence band is made up of Cu 3d electrons, a decrease in the intensity of the spectrum representing valence band edge is expected with increase in x (Cu vacancies) due to depletion of electrons from the valence band. Fig. 4(i) shows the difference spectra obtained by subtracting the intensity of the valence band peak of $Cu_{2-x}Zn_{1.3}SnS_4$ (x = 0.3, 0.5 and 0.7) from x = 0.0 spectrum. It can be clearly observed that the intensity of the difference spectra reduces when subtracted from x = 0.0 gradually. This creates curiosity to look at absorption spectra of $Cu_{2-x}Zn_{1.3}SnS_4$ (x = 0.0, 0.3, 0.5 and 0.7).

(b) When light is incident on the absorber layer, carriers in the valence band absorb energy and jump across the gap. When Cu vacancies are created in the valence band of the absorber, the available electrons are 'vacated' from the valence band; hence a reduction in the optical absorption is expected. The absorption spectra recorded on $Cu_{2-x}Zn_{1.3}SnS_4$ (x = 0.0, 0.3, 0.5 and 0.7) films is shown in Fig. 4(ii) It is evident that there is a clear fall in the absorption of the films for composition corresponding to x = 0.3, 0.5 and 0.7. For x = 0.0 there is a steady rise in the absorption with increase in energy, whereas for the other composition the increase in absorption is not that steady.

From the difference spectra of the valence band edge and reduced optical absorption, the role of Cu vacancies can be clearly observed. Since $|E_F - E_V|$ for any of the compositions in $Cu_{2-x}Zn_{1.3}SnS_4$ (x = 0.0, 0.3, 0.5 and 0.7) are not comparable to that of the bandgap of CZTS, it

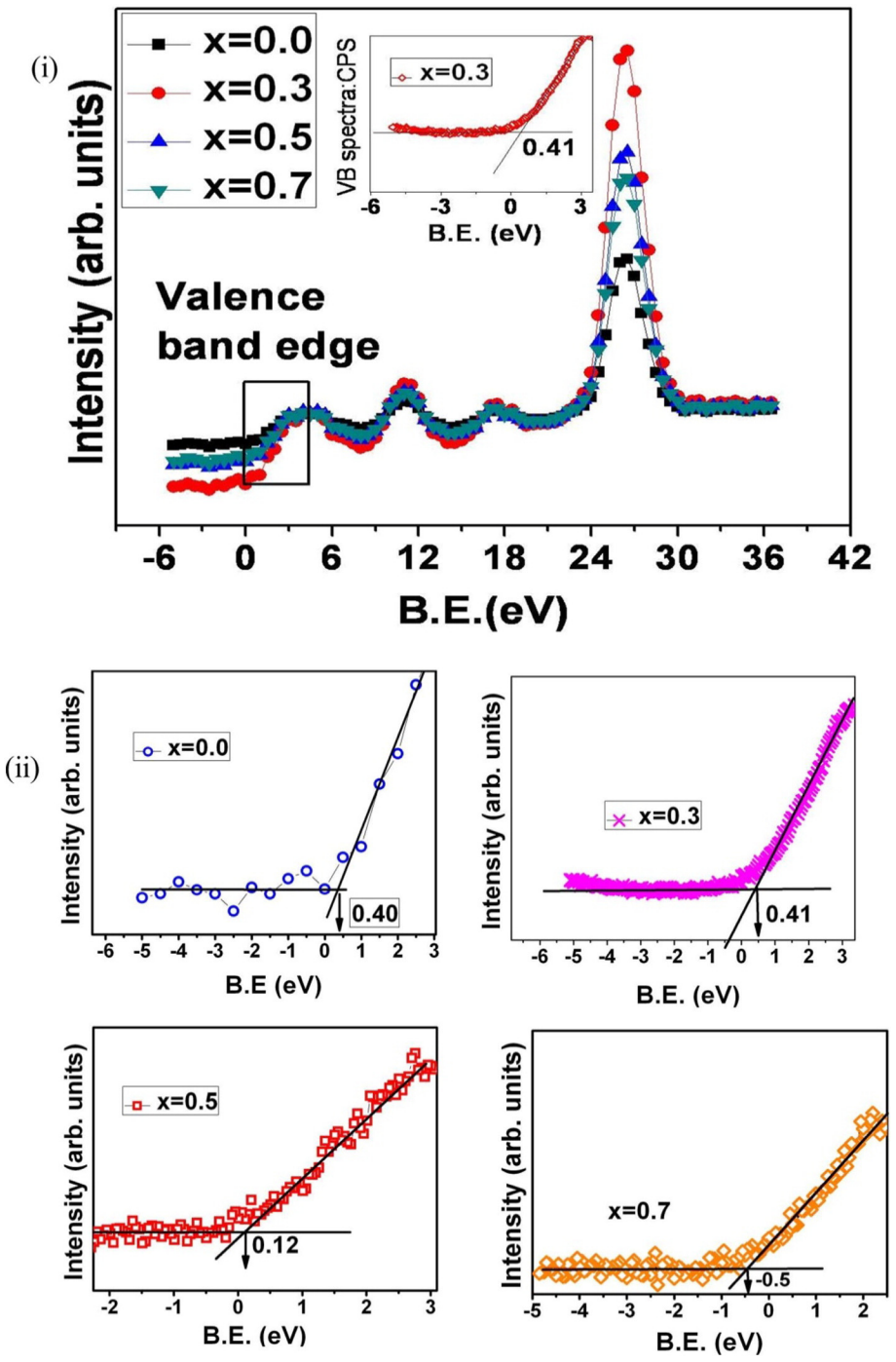

Fig. 2. (i). 0–30 eV range of total XPS spectra for $Cu_{2-x}Zn_{1.3}SnS_4$ (x = 0, 0.3, 0.5 and 0.7) films. The edge of the valence band is highlighted and it is determined for x = 0.3, (ii) Position of valence band edge determined for $Cu_{2-x}Zn_{1.3}SnS_4$ (a) x = 0.0, (b) x = 0.3, (c) x = 0.5 and (d) x = 0.7.

Table 1
$|E_F - E_V|$ values for different compositions along with Cu/(Zn + Sn) from EDS and (Zn + Sn)/(Zn + Sn + Cu) for the bulk and surface of the samples are listed.

$Cu_{2-x}Zn_{1.3}SnS_4$ x =	Cu/(Zn + Sn)	(Zn + Sn)/(Zn + Sn + Cu)		$\|E_F - E_V\|$	Bandgap E_g (eV)
		EDS	XPS		
0	1.0	0.39	0.82	0.32	1.48
0.3	0.74	0.51	0.79	0.41	1.63
0.5	0.65	0.59	0.83	0.07	1.58
0.7	0.57	0.69	0.89	0.50	1.31

confirms that in quaternary semiconductors like CZTS, formation of ordered vacancy compounds is not observed.

In addition to the formation of ordered vacancy compounds, Cu chalcogenides also exhibit unique GB physics. While the defect physics (formation of ordered vacancy compounds) is due to covalent and ionic nature of $CuInX_2$(X = S/Se) along with strong anti-bonding coupling between Cu 3*d* and S 3*p* electrons of valence and conduction bands respectively, unique GB physics arises due to catalyzing role of Na diffusing from sodalime glass substrate. There are several reports which explain the role of sodium diffusing from sodalime glass substrate into $CuInSe_2$ that plays crucial role in passivation of GBs and reduced recombination [21–23]. Sodium breaks O_2 molecule into O

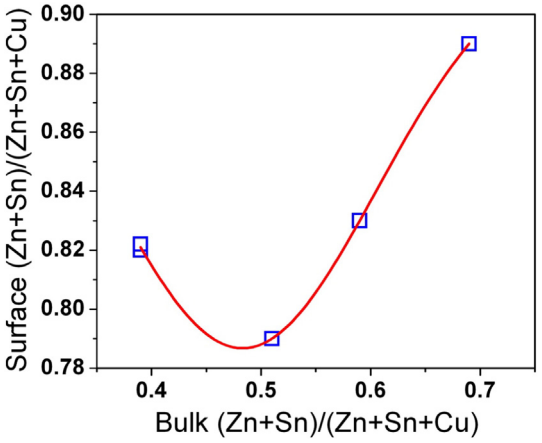

Fig. 3. (Zn + Sn)/(Zn + Sn + Cu) determined from XPS as a function of their values determined from EDS data.

atoms, these O atoms occupy S/Se vacancies and cleanup the mid bandgap states corresponding to S/Se vacancies [15,24]. While the hole barrier model explains how the holes are reflected from the grain boundaries, role of sodium explains how the mid-bandgap states are cleaned up [25]. Thus polycrystalline $CuInGaX_2$ (X = S, Se) (CIGS) solar cells show more efficiency than their single crystalline counter parts [17]. These aspects are well studied in ternary systems while in quaternary systems like Cu_2ZnSnS_4 (CZTS) it is still a matter of intense research [4,16,17,26,27]. Joel et al. have reported C-AFM studies on CZTS in order to measure the current at the interior of the grains and grain boundaries [4]. The present work discusses GB physics in CZTS deposited on sodalime glass coated with FTO and on Si (non-sodalime glass). For this purpose conductive atomic force microscopy (C-AFM) is utilized to obtain current maps along with topography images.

C-AFM studies were carried out on CZTS/Si and CZTS on sodalime glass substrates and the images are shown in Fig. S1 (b) and (c) respectively. Fig. S1(c) corresponds to topography of CZTS on Si.

Figs. S1 (b) and (c) correspond to current maps of CZTS films deposited on Si and FTO coated on sodalime glass. It is clear that the conductivity is more at the interior of grains compared to grain boundaries for CZTS on Si. The scale on the right side of the figures gives color code for maps indicating the spatial variation of current. For CZTS film deposited on Si, Fig. S1(b) dark brown region corresponds to regions of minimum current while light yellow or white regions correspond to regions with high current. It can be clearly observed from the current maps that in case of films deposited on Si, grain boundaries are regions corresponding minimum current whereas in case of films deposited on sodalime glass grain boundaries relatively higher current was observed. This clearly demonstrates that the model that explains grain boundary physics in ternary chalcogenides taking into account the role of sodium diffusing from the glass substrates also holds for quaternary semiconductors such as CZTS.

Further, C-AFM images were recorded for CZTS on Si at different bias voltages to check if there is any barrier voltage, above which grain boundaries become more conducting than the interior of grains. C-AFM images recorded at 0.4 V and 0.5 V of applied bias are shown in Fig. S2 (a) and (b) and no enhance current maps at grain boundaries were observed. Figs. S2(a) and (b) show the current maps recorded at 0.4 V and 0.5 V of applied.

A clear decrease in absorption shows Cu deficiency created in the valence band. Since $|E_F - E_V|$ for any of the composition is not comparable to bandgap, OVCs are not formed in CZTS. This could be one of the reasons for relatively lower efficiency of CZTS devices compared to CIGS. In case of CZTS deposited on sodalime glass, conductivity is more at the grain boundaries while in case of CZTS deposited on Si, conductivity at the interior of the grain is more. This shows the grain boundary physics that explains ternary chalcogenides is also applicable to quaternary CZTS.

Acknowledgment

The authors thank Department of Science and Technology (DST), New Delhi for facilitating the establishment of “Nano Functional Materials Technology Center” (Grant: SRNM/NAT/02–2005) at IIT Madras. The authors MSR and SKS are thankful for financial help obtained through the DST project (DST/TM/SERI/2K11/111).

Appendix A. Supplementary data

Supplementary data to this article can be found online at http://dx.doi.org/10.1016/j.scriptamat.2016.02.009.

References

[1] W. Wang, M.T. Winkler, O. Gunawan, T. Gokmen, T.K. Todorov, Y. Zhu, D.B. Mitzi, Adv. Energy Mater. 4 (2014) (n/a-n/a).
[2] W. Hsu, C.M. Sutter-Fella, M. Hettick, L. Cheng, S. Chan, Y. Chen, Y. Zeng, M. Zheng, H.-P. Wang, C.-C. Chiang, A. Javey, Sci. Rep. 5 (2015) 16028.
[3] A. Walsh, S. Chen, S.H. Wei, X.G. Gong, Adv. Energy Mater. 2 (2012) 400–409.
[4] J.B. Li, V. Chawla, B.M. Clemens, Adv. Mater. 24 (2012) 720–723.
[5] J. Kim, S. Kim, C.-S. Jiang, K. Ramanathan, M.M. Al-Jassim, Appl. Phys. Lett. 104 (2014) 063902.
[6] M. Edoff, Ambio 41 (2012) 112–118.
[7] L. Yin, G. Cheng, Y. Feng, Z. Li, C. Yang, X. Xiao, RSC Adv. 5 (2015) 40369–40374.
[8] V. Kosyak, N.M. Amiri, A. Postnikov, M. Scarpulla, J. Appl. Phys. 114 (2013) 124501.
[9] D.B. Mitzi, O. Gunawan, T.K. Todorov, K. Wang, S. Guha, Sol. Energy Mater. Sol. Cells 95 (2011) 1421–1436.
[10] J. Just, D. Lützenkirchen-Hecht, R. Frahm, S. Schorr, T. Unold, Appl. Phys. Lett. 99 (2011) 262105.
[11] A. Shavel, D. Cadavid, M. Ibanez, A. Carrete, A. Cabot, J. Am. Chem. Soc. 134 (2012) 1438–1441.

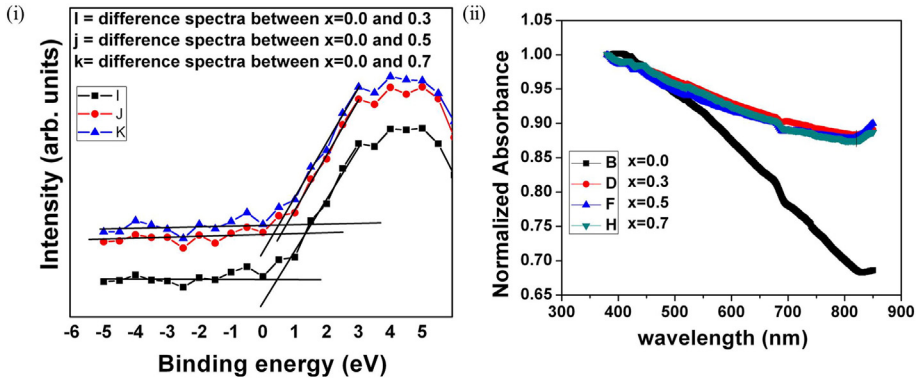

Fig. 4. (i). Difference spectra obtained by subtracting the intensity of valence band edge of $Cu_{2-x}Zn_{1.3}SnS_4$ (x = 0.3, 0.5 and 0.7) from x = 0.0 composition, (ii) absorption spectra of $Cu_{2-x}Zn_{1.3}SnS_4$ (x = 0.0, 0.3, 0.5 and 0.7) recorded in the visible region.

[12] Q. Guo, G.M. Ford, H.W. Hillhouse, R. Agrawal, Nano Lett. 9 (2009) 3060–3065.
[13] Q. Guo, G.M. Ford, W.-C. Yang, B.C. Walker, E.A. Stach, H.W. Hillhouse, R. Agrawal, J. Am. Chem. Soc. 132 (2010) 17384–17386.
[14] J.J. Scragg, J.T. Watjen, M. Edoff, T. Ericson, T. Kubart, C. Platzer-Björkman, J. Am. Chem. Soc. 134 (2012) 19330–19333.
[15] Y. Yan, C.-S. Jiang, R. Noufi, S.-H. Wei, H. Moutinho, M. Al-Jassim, Phys. Rev. Lett. 99 (2007) 235504.
[16] S. Zhang, S.-H. Wei, A. Zunger, Phys. Rev. Lett. 78 (1997) 4059.
[17] C. Persson, A. Zunger, Appl. Phys. Lett. 87 (2005) 211904.
[18] D. Schmid, M. Ruckh, F. Grunwald, H.-W. Schock, J. Appl. Phys. 73 (1993) 2902–2909.
[19] A. Klein, W. Jaegermann, Appl. Phys. Lett. 74 (1999) 2283.
[20] H. Du, M. Romero, I. Repins, G. Teeter, R. Noufi, M. Al-Jassim, Photovoltaic Specialists Conference (PVSC), 2011 37th IEEE, IEEE, 2011 001983–001986.
[21] L. Kronik, D. Cahen, H.W. Schock, Adv. Mater. 10 (1998) 31–36.
[22] P.T. Erslev, J.W. Lee, W.N. Shafarman, J.D. Cohen, Thin Solid Films 517 (2009) 2277–2281.
[23] J.-F. Guillemoles, L. Kronik, D. Cahen, U. Rau, A. Jasenek, H.-W. Schock, J. Phys. Chem. B 104 (2000) 4849–4862.
[24] S.-H. Wei, S.B. Zhang, A. Zunger, J. Appl. Phys. 85 (1999) 7214–7218.
[25] C. Li, Y. Wu, J. Poplawsky, T.J. Pennycook, N. Paudel, W. Yin, S.J. Haigh, M.P. Oxley, A.R. Lupini, M. Al-Jassim, Phys. Rev. Lett. 112 (2014) 156103.
[26] J.E. Jaffe, A. Zunger, Phys. Rev. B 64 (2001) 241304.
[27] C. Persson, A. Zunger, Phys. Rev. Lett. 91 (2003) 266401.